Supporting Information

Pinkney et al. 10.1073/pnas.1211922109

SI Text

DNA and Protein Preparation. Mutants of Cre were prepared with QuikChange Site-Directed Mutagenesis Kit (Stratagene), and tagless proteins were purified, according to Ghosh et al. (1), and their identities were confirmed with mass spectroscopy. A total of 1,087 bp DNA substrates were prepared via a PCR using two fluorescently labeled oligonucleotides as primers and a plasmid template containing directly repeated *loxP* sites separated by a 1 kb Km^R gene (pRB10*loxP*) and Phusion High-Fidelity DNA polymerase (NEB). Two oligonucleotides were used: forward 5′-tgcatgcgatatcaX-aacttcgtat-3′ and reverse 5′-gtggatccacXtgataacttcgtat-3′, where X indicates the position of 5-C6-amino dT; additionally, the 5′ end of the reverse oligonucleotide was labeled with biotin. Forward and reversed oligonucleotides were labeled at X positions with Cy5 and Cy3B, respectively. Oligonucleotides were synthesized and HPLC purified by ATDBio Ltd. Cy5 labeling was performed by ATDBio, whereas Cy3B labeling was performed as previously described (2). After PCR reactions, the product was gel-purified.

Instrumentation. Single-molecule TIRF experiments were performed on a custom-built objective type TIRF microscope. A green (532 nm Cobolt Samba) and red (635 nm Cube Coherent) laser were combined using a dichroic mirror and coupled into a fiber optic cable. The output of the fiber was focused into the back focal plane of the objective (100× oil immersion, numerical aperture 1.4, Olympus) and displaced perpendicular to the optical axis such that laser light was incident at the slide-solution interface at greater than the critical angle, creating an evanescent excitation field. ALEX (2) was implemented by directly modulating the lasers, and all data were acquired using a 100 Hz alternation rate, with excitation powers of 1 mW for each laser. Fluorescence emission was collected by the objective and separated from the excitation light by a dichroic (545 nm / 650 nm, Semrock) and cleanup filters (545 nm LP, Chroma; and 633/25 nm notch filter, Semrock). Emission signal was focused on a rectangular slit to crop the image and then spectrally separated, using a dichroic (630 nm DRLP; Omega), into two emission channels which were focused side by side onto an EMCCD camera (Andor iXon 897). The EMCDD was set to an EM gain of 300, corresponding to an approximate real gain of 4.55 counts per photon.

Sample Preparation. Biotinylated DNA was immobilized to the surface of a PEG-passivated coverslip using biotin–neutravidin interactions and sealed using a silicone gasket (Grace Bio-laboratories) and a second coverslip as a lid. Imaging was performed in a buffer consisting of 50 mM Tris·HCl (pH 7.5), 50 mM NaCl, 5 mM $MgCl_2$, 100 μg·mL^{-1} BSA, and 1 mM UV-treated Trolox. An enzymatic oxygen scavenging system consisting of 1 mg·mL^{-1} glucose oxidase, 40 μg·mL^{-1} catalase, and 1.4% (wt/vol) glucose was added just before sealing the sample before image acquisition. All experiments were performed at a room temperature of 21 °C. In experiments where SDS was used to disrupt protein interactions, it was added to the buffer at a concentration of 0.1%.

Data Analysis. Extraction of fluorescence intensity signals from microscope images was performed by the previously described TwoTone software (3). An apparent FRET efficiency, E^*, was calculated from the extracted fluorescence emission:

$$E^* = \frac{F_{DA}}{F_{DD} + F_{DA}},$$

and the acceptor PSF width was obtained from the mean width of the fitted elliptical Gaussian.

Further analysis and quantification of extracted signals was performed with custom-written MATLAB software. For analysis of recombination events, intensity traces from individual molecules was manually inspected and classified. Transient FRET signals were defined on the basis of $E^* > 0.2$ along with the appropriate changes in PSF width and acceptor intensity; in the case of events that returned to substrate, short events (less than two frames) were discarded as these could not reliably be distinguished from fluctuations due to noise. However, in the case of "productive" events, unambiguous PSF and intensity signals allowed assignment of events that displayed short or no transient FRET. Any molecules whose fluorophores bleached within 10 s of a FRET event or that exhibited confounding photophysical fluctuations were excluded from the analysis. Under our imaging conditions, we measure the lifetimes of Cy3B and Cy5 to be ∼400 s and 160 s, respectively (fit to single exponential decay), and that ∼10% of molecules show errant photophysics from either fluorophore. Further, ∼5% of molecules were observed with two-step photobleaching or intensities corresponding to more than one fluorophore at a single localization position, and these were discarded.

Histograms of E^* values were constructed by extracting the manually assigned FRET frames, discarding the first and last frames, and plotting the data points to a histogram, normalizing each count by the length of the observed event.

FCS Experiments. FCS was carried out on a ConfoCor 3 system (Carl Zeiss). The 633 nm line of a HeNe laser was directed via 488/561/633 dichroic mirror and focused with a Zeiss C-Apochromat 40× NA 1.2 water immersion objective to excite experimental samples containing Cy5. Fluorescence emission was collected using a 655-nm longpass filter and recorded by a set of avalanche photodiodes. The pinhole diameter was adjusted to 83 μm (one Airy unit), and the pinhole position was optimized with use of the automatic pinhole adjustment for Cy5.

FCS measurements were conducted for BS FRET substrate (Fig. S2*A*) in the presence of 0.05% SDS as well as without the detergent. The SDS concentration used was below the cpc (critical micelle concentration = 8.15×10^{-3} M, whereas the 0.05% SDS used in our studies corresponds to 1.7×10^{-3} M), and we did not observe any change in diffusion upon SDS addition.

To acquire kinetics of the recombination reaction and dissociation of product DNAs, we performed reactions in solution where 2 nM of the BS FRET substrate were mixed with 320 nM Cre protein. To avoid rebinding of short product DNA back to the BS FRET substrate, an excess of a *loxP* containing short oligonucleotide (100 nM) was present as a competitor. It should be noted that in the case of intermolecular reactions between the BS FRET substrate and short oligonucleotide, the resulting product will have very similar length to that produced by intramolecular reactions (58 bp and 60 bp, respectively), which will have no appreciable effect on the change in diffusion time. During the course of the experiment, decrease in diffusion time was analyzed as a function of product dissociation after completion of recombination. It is worth noting that only molecules that completed all chemistry steps and then dissociated would result in a decreased diffusion time, whereas nonproductive synaptic complexes and reactions stuck at the HJ stage would have no effect. To analyze the stability of a complex after all chemistry was completed, we prepared a volume of 500 μL

of the reaction mixture containing Cre, BS FRET substrate, and oligonucleotide. Then a 50 μL volume was put in a glass chamber to perform 60× 1-min FCS measurements. The rest of the mixture was used to analyze the change in diffusion coefficient using SDS to disrupt any protein–protein and protein–DNA interactions. Any difference in diffusion time between samples quenched with SDS and those in native conditions would be the result of stability of product DNA before dissociation. For this purpose 19 μL was taken from the reaction mixture and stopped by addition of 1 μL 1% SDS. The Cre-*loxP* reaction was stopped minute-by-minute for the first 10 min, then at 15, 20, 30, 40, 50, and 60 min of incubation in 22 °C. The reference sample used to calculate diffusion coefficient was BS FRET substrate with SDS.

Samples quenched with SDS were measured 5 × 10 s. All FCS experiments were carried out in Lab-Tek (Nagle Nunc International) eight-well chambered borosilicate glass plates at 22 ± 1 °C.

FCS Data Analysis. In FCS experiments the intensity of fluorescence signal is measured and the autocorrelation function $G(\mathrm{t})$ is determined for diffusing fluorophores present in the sample. Here, $G(\mathrm{t})$ can be expressed as a two-component model (4):

$$G(\tau) = \left[1 - T + T\exp\left(\frac{-\tau}{\tau_T}\right)\right]N^{-1} \times \left[\frac{1-Y}{\left(1+\frac{\tau}{\tau_{substrate}}\right)\sqrt{1+\frac{r_0^2}{z_0^2}\frac{\tau}{\tau_{substrate}}}} + \frac{Y}{\left(1+\frac{\tau}{\tau_{product}}\right)\sqrt{1+\frac{r_0^2}{z_0^2}\frac{\tau}{\tau_{product}}}}\right],$$

where T is the average fraction of dye molecules in the triplet state with the relaxation time τ_T, N is the average number of fluorescent molecules in the volume observed, Y is the relative fraction of released product DNA, $\tau_{substrate}$ and $\tau_{product}$ are the diffusion time constants of substrate DNA and product DNA, respectively, and r_0 and z_0 are the lateral and axial dimension respectively of the observation volume. The diffusion coefficient can be determined by calibrating the experiment using a standard dye, in our case Cy5 ($D = 3.7 \times 10^{-6}$ $cm^2 \cdot s^{-1}$; ref. 5). Diffusion coefficients for any labeled DNA can then be calculated according to the relation:

$$D_x = \frac{\tau_{Cy5}}{\tau_x} D_{Cy5},$$

where D_{Cy5} is the diffusion coefficient,τ_{Cy5} is the correlation time of Cy5 (55 μs), and D_x and τ_x are the diffusion coefficient and correlation time for the labeled DNA. We calculated diffusion coefficients of the BS FRET substrate and product DNA to be 0.24×10^{-6} $cm^2 \cdot s^{-1}$ and 0.92×10^{-6} $cm^2 \cdot s^{-1}$, respectively.

The correlation time of the BS FRET substrate was determined assuming a one-component model. The correlation time of the product DNA was obtained by fitting an overnight recombination reaction stopped with SDS to a two-component model with fixed time for BS FRET substrate and the second component left free. During the analysis of experiments, the correlation times for BS FRET substrate and product DNA were fixed at measured values. All of the calculations, including the evaluation of the autocorrelation curves, which was carried out with a Marquardt nonlinear least-square fitting procedure, were performed using the software of the ConfoCor 3 instrument.

Quantifying Complex Formation Frequency. To quantify the frequency of complex formation events we calculate a probability of complex formation per particle, by dividing the total number of events observed by the initial number of substrate molecules in a given movie. To account for the varying length of our movies, for example due to cessation caused by focal drift, we divide this probability by the mean movie length to obtain an approximate probability of complex formation per particle per unit time. This calculation assumes that all substrate molecules are available to participate in reactions and that photo-bleaching is not a major factor over the timescales for which we observe. These assumptions likely do not hold for our surface-immobilized DNAs and 100-s movies, so we cannot use this probability to accurately infer information about the absolute on-rate of complex formation. However, the above effects are equivalent over all our experimental conditions, so we can reliably compare this value between experiments to determine the relative frequency of complexes formed. We also note that very short-lived synaptic complexes are likely to be missed due to our temporal resolution of 100 ms; thus, the probability values given in the case of synaptic complex formation are likely to be lower limits.

Accurate FRET and Distance Calculation. We follow previously described procedures for obtaining accurate FRET (6). Briefly, we correct for donor leakage into the acceptor emission channel, l; direct excitation of the acceptor by the 532 nm laser, d; and the effect of differing quantum yields Q, and detection efficiency η, of the fluorophores, generally termed γ, to give an expression for accurate FRET given by:

$$E = \frac{DA_{correct}}{\gamma F_{DD}(1+l) + DA_{correct}},$$

where:

$$DA_{correct} = F_{DA} - lF_{DD} - dF_{AA},$$

and:

$$\gamma = \frac{Q_A \eta_A}{Q_D \eta_D}.$$

We obtain values for l and d by looking at fluorescence signals from the appropriate singly labeled short oligonucleotides. The ratio γ is determined by measuring many acceptor bleaching during FRET events observed with Cre A312T (7); the mean of these single measurements for γ is then used as a correction for all molecules.

Emission spectra of Cy3B and absorption spectra of Cy5 were measured on a fluorometer (Photon Technology International) under conditions as closely resembling those of the single-molecule experiment as possible. R_0 was calculated using the expression:

$$R_0 = 0.211(\kappa^2 n^{-4} Q_D J)^{1/6},$$

$$J = \int f_D(\lambda)\varepsilon_A(\lambda)\lambda^4 d\lambda,$$

where n is the refractive index of the medium (1.33), f_D is the normalized fluorescence emission of the donor, and ε_A is the extinction coefficient of the acceptor. We assume a literature value of 0.67 for Q_D, the quantum yield of Cy3B (8), and that the dipole orientation factor $\kappa^2 = 2/3$. To justify our assumption of rotational freedom of the fluorophores attached to DNA, we measure their anisotropy values in the presence of wt Cre and use these to obtain an estimate for the possible range of true values for κ^2 (9). We use these errors, and the SD of our E^* and stoichiometery values, as well as estimates for the errors on the measurements of fluo-

rophore spectral properties, to perform standard propagation of errors to compute the SEM for our distance measurements, as outlined in Uphoff et al. (10) (Table S2).

To estimate the expected interfluorophore distance we extrapolate one DNA arm of the Cre-*loxP* synaptic complex structure [2HOI (11) for the BS conformation and 1 NZB (12) for the TS conformation] to encompass our labeling site. To account for the effect of linker length, we superimpose the sterically accessible region computed by Wozniak et al. (13) and use the mean fluorophore positions to estimate their separation.

Post-recombination Synaptic Complex Distance. The distance estimate from crystal structures of the TS-HJ and TS-P complex are 83 Å; measuring the FRET value after the BS complex in our "productive" complexes, we obtain a mean value of 0.18, indicating a distance of 84 ± 11 Å. Although this is measurable over the ensemble of single molecules, we refer to this as a "negligible" FRET value due to its proximity to the FRET efficiency arising solely due to spectral crosstalk in our system ($E^* = 0.13$), and consequently it is not reliably identifiable in intensity traces from individual molecules.

FRET Simulations. Simulations were performed assuming rapid interconversion between the two HJ conformers to determine if this could give rise to the observed FRET distributions. We simulated stochastic fluorophore emission from two states that were able to interconvert faster than the frame time of acquisition using a Markov chain approach; we assigned these states to have uncorrected FRET values of 0.18 and 0.43 for the TS-HJ and BS-HJ, respectively, estimated from the 2HOI crystal structure (11). The fluorescence emission collected over a frame was then put through simulated background noise and EM gain to obtain the final emission counts in simulated data. We tune the rate of fluorophore photon emission in the simulations to produce distributions that match the observed width arising from a static FRET standard. This gives rise to photon counts that are somewhat lower than those from single molecules in our experiments to reproduce the effect of broadening due to collating an ensemble of single molecules in our FRET distributions (3).

To obtain an estimate for the rates of interconversion that could recapitulate the observed distribution, we systematically varied the forward and backward rates of HJ interconversion (Fig. S6) and performed many simulated runs for each parameter pair for a number of frames corresponding to those in the experimental data. We then fitted the output distribution using a single Gaussian and recorded the mean, variance, and the coefficient of determination of the fit. Assuming a normal distribution of parameter values for each model, we then computed the likelihood of the model given our observed data (Fig. S5). By the definition of likelihood, the parameters that maximized this value would be those that are most likely to give rise to our observed data.

1. Ghosh K, Van Duyne GD (2002) Cre-loxP biochemistry. *Methods* 28(3):374–383.
2. Kapanidis AN (2008) Alternating-laser excitation of single molecules. *Single Molecule Techniques: A Laboratory Manual*, eds Selvin PR, Ha T (Cold Spring Harbor Laboratory Press, Cold Spring Harbor, NY), 1st Ed, pp 85–119.
3. Holden SJ, et al. (2010) Defining the limits of single-molecule FRET resolution in TIRF microscopy. *Biophys J* 99(9):3102–3111.
4. Meyer-Almes FJ, Wyzgol K, Powell MJ (1998) Mechanism of the alpha-complementation reaction of E. coli beta-galactosidase deduced from fluorescence correlation spectroscopy measurements. *Biophys Chem* 75(2):151–160.
5. Loman A, Dertinger T, Koberling F, Enderlein J (2008) Comparison of optical saturation effects in conventional and dual-focus fluorescence correlation spectroscopy. *Chem Phys Lett* 459:18–21.
6. Lee NK, et al. (2005) Accurate FRET measurements within single diffusing biomolecules using alternating-laser excitation. *Biophys J* 88(4):2939–2953.
7. Ha T, et al. (1999) Single-molecule fluorescence spectroscopy of enzyme conformational dynamics and cleavage mechanism. *Proc Natl Acad Sci USA* 96(3):893–898.
8. Cooper M, et al. (2004) Cy3B: Improving the performance of cyanine dyes. *J Fluoresc* 14(2):145–150.
9. Dale RE, Eisinger J, Blumberg WE (1979) The orientational freedom of molecular probes. The orientation factor in intramolecular energy transfer. *Biophys J* 26(2):161–193.
10. Uphoff S, et al. (2010) Monitoring multiple distances within a single molecule using switchable FRET. *Nat Methods* 7(10):831–836.
11. Ghosh K, Guo F, Van Duyne GD (2007) Synapsis of loxP sites by Cre recombinase. *J Biol Chem* 282(33):24004–24016.
12. Ennifar E, Meyer JEW, Buchholz F, Stewart AF, Suck D (2003) Crystal structure of a wild-type Cre recombinase-loxP synapse reveals a novel spacer conformation suggesting an alternative mechanism for DNA cleavage activation. *Nucleic Acids Res* 31(18):5449–5460.
13. Wozniak AK, Schröder GF, Grubmüller H, Seidel CAM, Oesterhelt F (2008) Single-molecule FRET measures bends and kinks in DNA. *Proc Natl Acad Sci USA* 105(47): 18337–18342.

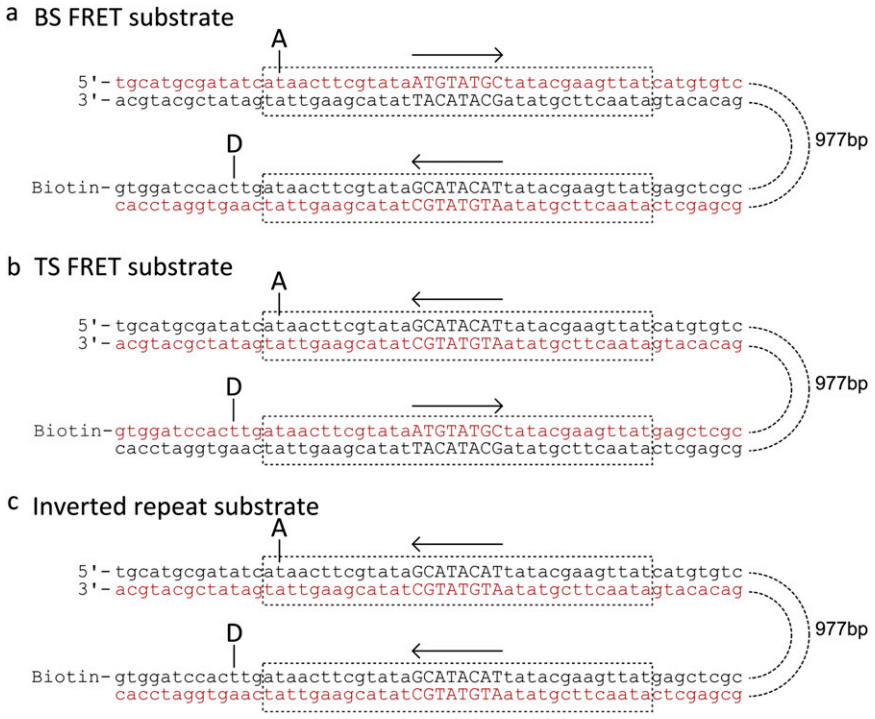

Fig. S1. Sequences and labeling positions of DNA substrates used throughout this study. (*A*) BS FRET substrate, designed to show FRET in the BS-S complex. (*B*) TS FRET substrate, designed to show FRET in the TS-S complex. (*C*) Inverted repeat substrate, used to investigate complex dissociation. *loxP* sites are indicated by dashed boxes, and the orientation by the arrows above. TSs and BSs are indicated in red and black, respectively; the long sequence of DNA linking the sites is not shown and is represented by dashed lines.

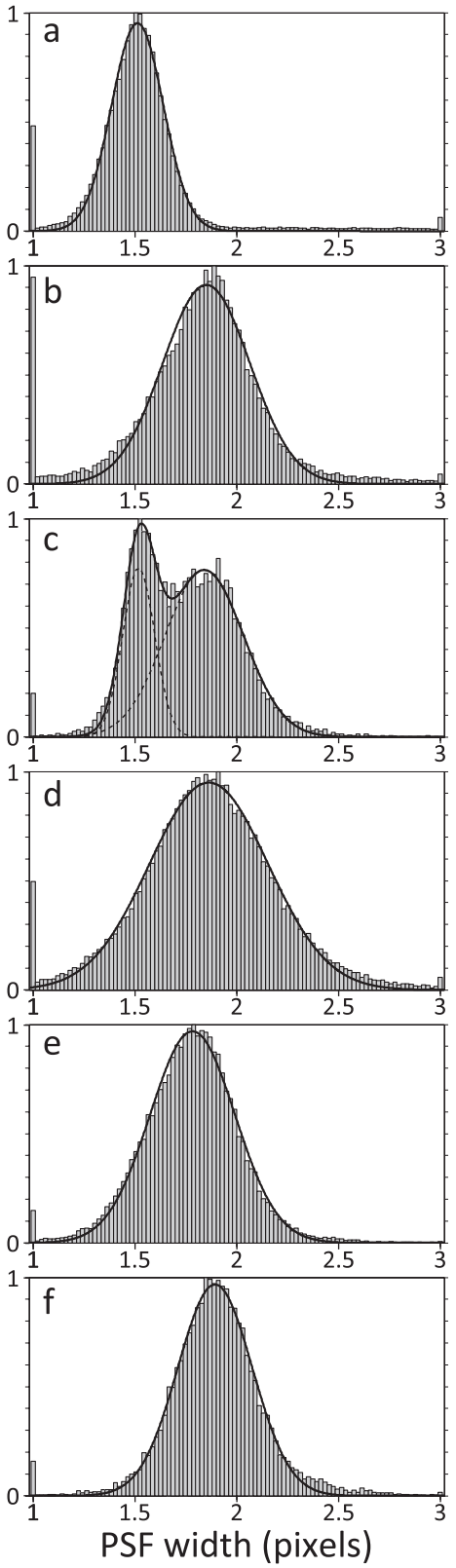

Fig. S2. End point assay to verify recombination proficiency of molecules tethered to a PEG passivated coverslip. (*A*) Short (80 bp) labeled DNA, (*B*) long (1 kb) substrate DNA molecules with no protein to act as length standards, (*C–F*) Long substrate DNA incubated with proteins: *C*, wt Cre; *D*, Cre K201A; *E*, Cre A312T; *F*, Cre A36V for 10 min at room temperature (22 °C). Samples were then washed with buffer, SDS, and buffer again before a final wash with imaging buffer, after which 500-frame movies from five fields of view were collected to sample the state of molecules at the surface; *A* shows the typical diffraction-limited PSF expected for a surface-immobilized fluorophore on the microscope; (*B* and *D–F*) exhibit broadening concomitant with the long DNA substrate; and *C* shows a mix of broad and narrow PSFs, indicating that ~30% of surface-immobilized molecules have undergone at least one pair of strand exchange.

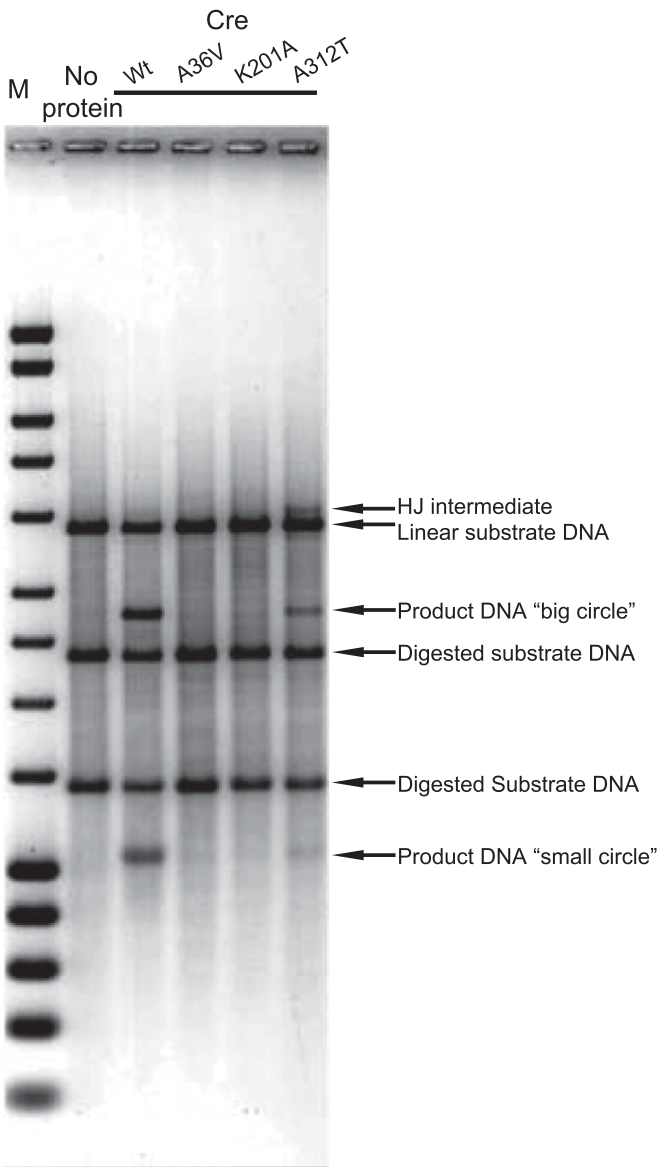

Fig. S3. Gel electrophoresis of recombination reaction carried for 10 min at 37° in buffer used thorough all studies. A 3.7 kb plasmid caring two directly repeated *loxP* sites (used as a template in PCR) was used. Product of recombination is expected to be “big” (2.7 kb) and “small” (1 kb) circles. Double digest reveal linearized products in reaction with wt and A312T mutant but none when A36V or K201A was used. As expected, A312T is less efficient in recombination and accumulates HJ intermediate.

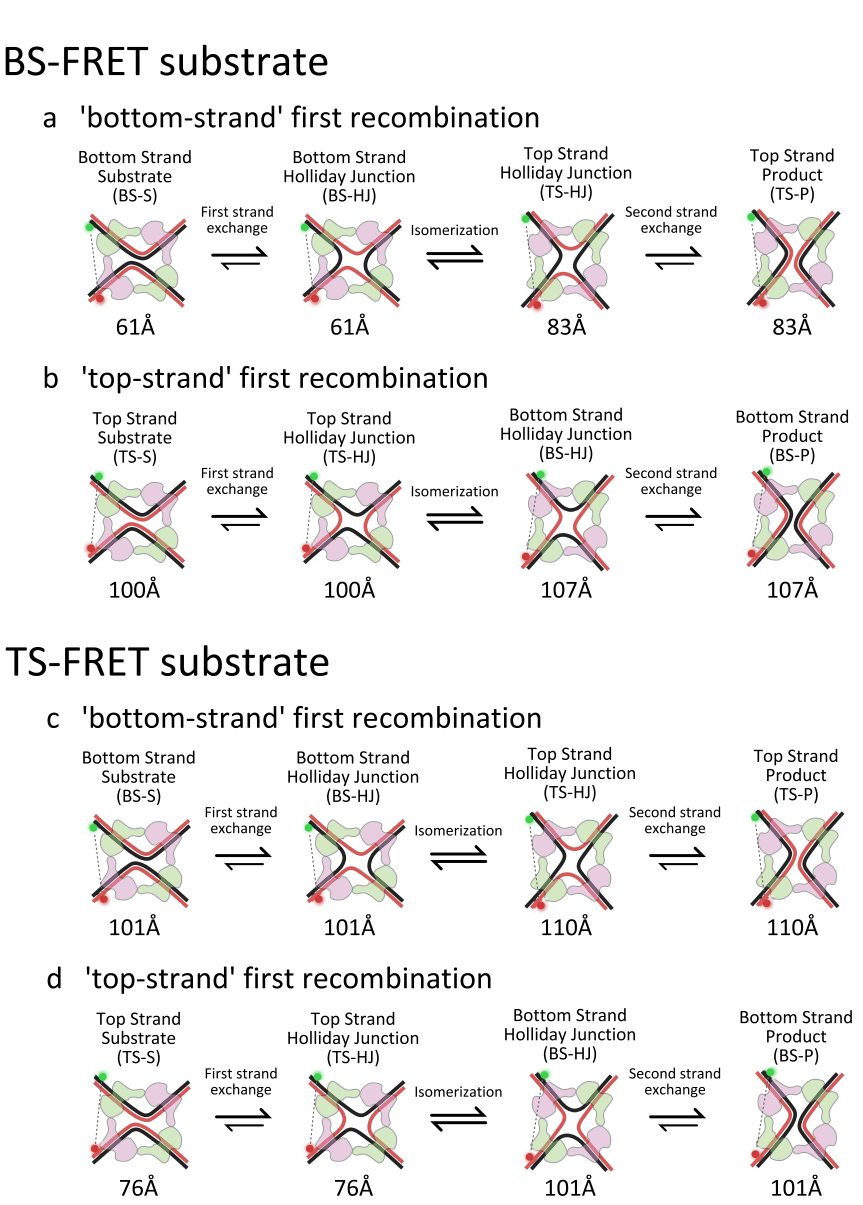

Fig. S4. Schematic comparison of the expected interfluorophore distances (as measured from crystal structures) at each stage of the reaction using either the BS-FRET substrate (*A* and *B*) or the TS-FRET substrate (*C* and *D*). For each substrate two possible reaction paths are shown: reactions can either be initiated from a substrate in which BSs are positioned to be cleaved first (*A* and *C*) or one in which TSs are cleaved first (*B* and *D*).

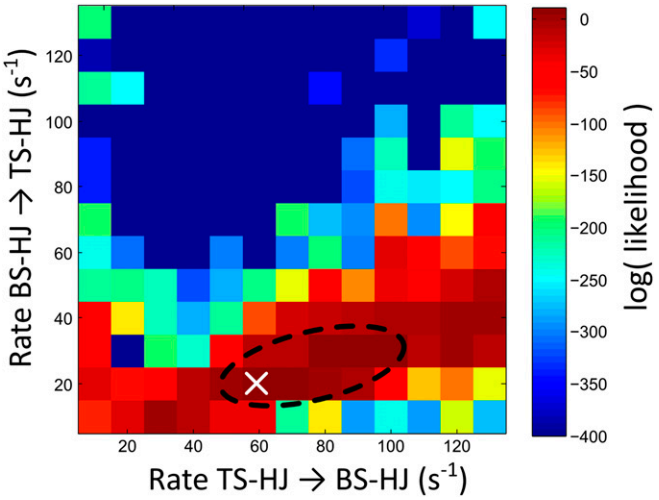

Fig. S5. Likelihood of the observed data given the distributions obtained from simulating many observations with a forward and backward rate of interconversion between HJ isomers (*SI Text*). The region of the graph giving the maximum likelihood values is outlined in black, and the pair of rates giving the maximum value is marked with a white cross.

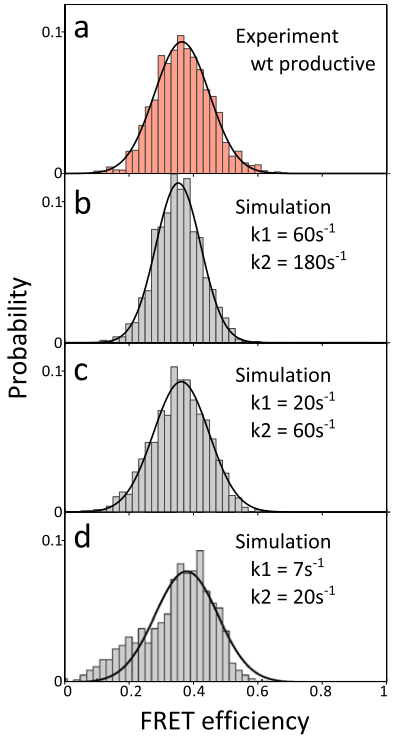

Fig. S6. Comparison of FRET efficiency distributions. (*A*) experimental wild-type Cre productive complex distribution and (*B–D*) simulated data with varying forward and backward rates of interconversion between the two HJ isomers.

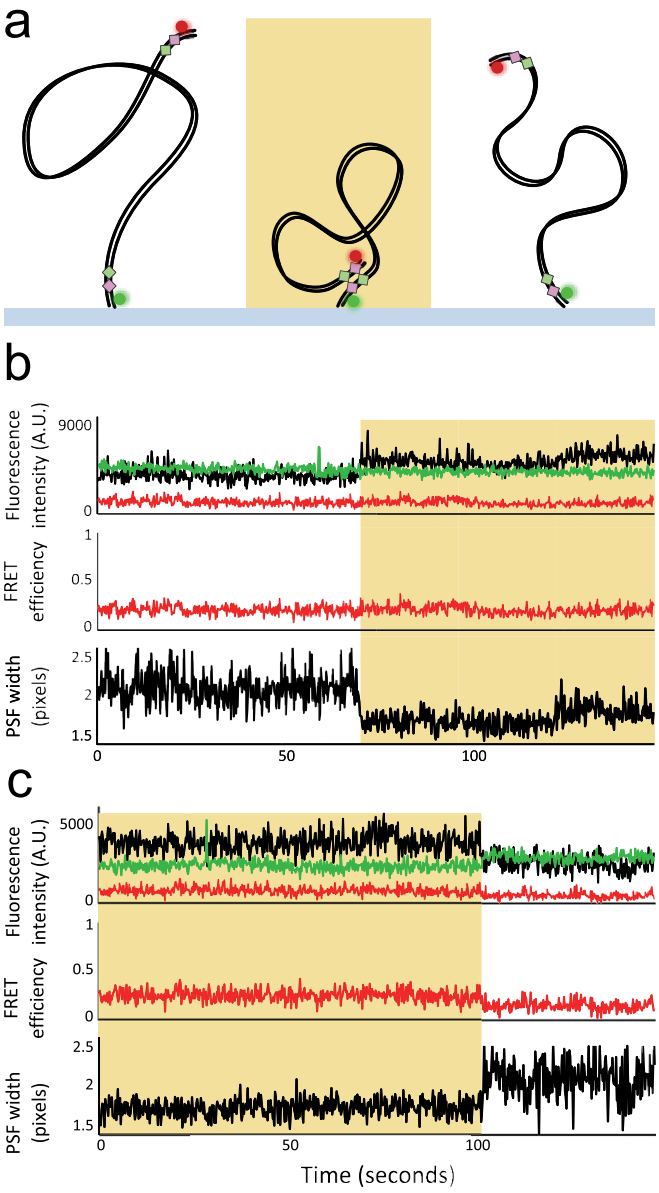

Fig. S7. Using an alternative substrate to assess the stability of the recombinant product complex. (*A*) Schematic of substrate used with *loxP* sites in an inverted arrangement. BS-S complex formation leads to a decrease in PSF width but no FRET. Recombination results in the inversion of the DNA linking the two *loxP* sites of the substrate, and dissociation of the product complex leads to a return to high PSF. (*B*) Example time trace of a single substrate molecule undergoing complex formation. (*C*) Time trace from a separate molecule showing dissociation of a complex to a long DNA, which we attribute to dissociation of the recombinant product synaptic complex.

Table S1. Accurate FRET efficiencies and the corresponding distances from populations fitted to histograms in Fig. 3

Population	Accurate FRET	SD	Distance (Å)	SD
wt, productive	0.58	0.07	67	5
wt, nonproductive (high)	0.65	0.06	64	5
wt, nonproductive (low)	0.42	0.10	75	7
A36V	0.62	0.09	65	6
A312T	0.64	0.07	64	5
K201A	0.44	0.11	74	7

Table S2. Fit parameters of width and SD for the Gaussian fits to histograms in Fig. 3

Population	Mean	SEM	SD of the fit	SEM of the SD
wt, productive	0.36	0.013	0.085	0.006
wt, nonproductive (high)	0.43	0.015	0.065	0.008
wt, nonproductive (low)	0.26	0.023	0.057	0.011
A36V	0.42	0.018	0.067	0.009
A312T	0.42	0.021	0.073	0.011
K201A	0.28	0.009	0.056	0.004